Cancer Letters 495 (2020) 135–144

Contents lists available at ScienceDirect

Cancer Letters

journal homepage: www.elsevier.com/locate/canlet

Combined blockade of polo-like kinase and pan-RAF is effective against *NRAS*-mutant non-small cell lung cancer cells

Siyeon Park [a], Tae Min Kim [a,b,*], Sung-Yup Cho [a,c,d,**], Soyeon Kim [a,e], Yumi Oh [c], Miso Kim [a,b], Bhumsuk Keam [a,b], Dong-Wan Kim [a,b], Dae Seog Heo [a,b]

[a] Seoul National University Cancer Research Institute, South Korea
[b] Department of Internal Medicine, Seoul National University Hospital, South Korea
[c] Department of Biochemistry and Molecular Biology, Seoul National University College of Medicine, South Korea
[d] Department of Biomedical Sciences, Seoul National University College of Medicine, Seoul, South Korea
[e] Biomedical Research Institute, Seoul National University Hospital, Seoul, South Korea

ARTICLE INFO

Keywords:
NRAS-mutant lung cancer
High-throughput screening
Pan-RAF inhibitor
PLK1 inhibitor

ABSTRACT

NRAS mutation is rarely observed in non-small cell lung cancer (NSCLC) patients, and there are no approved treatments for *NRAS*-mutant NSCLC. Here, we evaluated the effect of pan-RAF inhibitors on human *NRAS*-mutant NSCLC cell lines and performed high-throughput screening using human kinome small interfering (si) RNA or CRISPR/Cas9 libraries to identify new targets for combination NSCLC treatment. Our results indicate that human *NRAS*-mutant NSCLC cells are moderately sensitive to pan-RAF inhibitors. High-throughput kinome screenings further showed that G2/M arrest, particularly following knockdown of polo-like kinase 1 (PLK1), can inhibit the growth of human *NRAS*-mutant NSCLC cells and those treated with the type II pan-RAF inhibitor LXH254. In addition, treatment with volasertib plus LXH254, resulting in dual blockade of PLK1 and pan-RAF, was found to be more effective than LXH254 monotherapy for inhibiting long-term cell viability, suggesting that this combination therapeutic strategy may lead to promising results in the clinic.

1. Introduction

Lung cancer is the leading cause of death globally, as well as in South Korea [1,2]. Non-small cell lung cancer (NSCLC) accounts for approximately 80% of lung cancer cases and harbors multiple targetable genomic alterations [1,3]. Targetable oncogenes identified in Korean patients with lung adenocarcinomas include EGFR-activating mutation (60%), *KRAS* mutation (12%), *NRAS* mutation (1.5%), and *BRAF* mutation (<1.0%) [4]. *NRAS* mutation has been observed in 0.7–1.2% of NSCLC patients [5–7], and therefore, sufficient clinical data in this NSCLC subtype remains lacking.

The RAS GTPase maintains cell survival, proliferation, and migration through RAF kinase activity [8]. Although *RAS* has been one of the most well-studied oncogenes over the past 30 years, drug development is limited due to the difficulty associated with producing molecules that bind to the flat structure of RAS. In addition, the strong GTP-binding affinity of Ras makes it challenging to interrupt this interaction, suggesting that RAS is "undruggable" [9]. Recently, *KRAS* G12C-specific inhibitors that bind to the flat structure of Ras have been developed, which show promising efficacy against $KRAS^{G12C}$-mutant NSCLC (e.g., AMG510; objective response rate of 50%) [10,11]. However, *NRAS*-mutant NSCLC often has distinct genetic alterations as compared to *KRAS*-mutant NSCLC. In particular, *KRAS*-mutant NSCLC is characterized by a large proportion of mutations in the G12 site within the p-loop domain that binds the GTP β-phosphate, whereas *NRAS*-mutant NSCLC mutations are mainly clustered in the Q61 site within the conserved switch I domain that functions in GTP hydrolysis [12]. Therefore, therapeutic strategies for treating *NRAS*-mutant cancer require a different approach from those used to treat *KRAS*-mutant cancer.

In most *RAS*-mutant cancers, tumor growth can be inhibited by blocking the RAF-MEK-ERK pathway or other molecules downstream of RAS. Further, although BRAF-specific inhibitors are effective against $BRAF^{V600E/K}$-mutant cancers, they are ineffective for treating *RAS*-mutant cancers due to activation of RAF1 and ARAF [13]. Recently,

* Corresponding authors. Department of Internal Medicine, Seoul National University Hospital, 101 Daehak-ro, Jongno-gu, Seoul, 03080, Republic of Korea.
** Corresponding author. Department of Biochemistry and Molecular Biology, Seoul National University College of Medicine, 103 Daehak-ro, Jongno-gu, Seoul, 03080, Republic of Korea.
E-mail addresses: gabriel9@snu.ac.kr (T.M. Kim), csybio@snu.ac.kr (S.-Y. Cho).

https://doi.org/10.1016/j.canlet.2020.09.018
Received 14 March 2020; Received in revised form 11 September 2020; Accepted 19 September 2020
Available online 23 September 2020

pan-RAF inhibitors that prevent paradoxical feedback and theoretically target *RAS*-mutant cells were developed. Belvarafenib, a novel type II pan-RAF inhibitor, was found to exhibit an objective response rate of 44.4% in patients with *NRAS*-mutant melanoma [14]. In addition, LY3009120, which blocks activation of RAF dimers [15], was shown to be preclinically effective for *RAS*-mutant cancers, particularly *NRAS*--mutant melanoma and *KRAS*-mutant lung cancer, mainly by promoting disease stabilization in a Phase 1 study [16]. LXH254, a type II pan-RAF inhibitor with high selectivity for BRAF and CRAF, has shown anti-tumor activity in preclinical *NRAS*-mutant models and is currently being investigated in a Phase 1 study in patients with solid tumors harboring MAPK pathway alterations [17]. In this study, we aimed to evaluate the efficacy of pan-RAF inhibitors against *NRAS*-mutant cells *in vitro* and uncover an ideal combination strategy for *NRAS*-mutant NSCLC using high-throughput kinome screening.

2. Materials and methods

2.1. Patient, cell lines, and reagents

A 77-year-old male diagnosed with metastatic NSCLC harboring the *NRAS* G13R mutation received 800-mg LXH254 once daily (NCT02607813) and showed stable disease for 10 months with symptomatic improvement (Supplementary Fig. S1).

All patient-derived NSCLC cell lines were purchased from the Korean Cell Line Bank (Seoul, South Korea) and maintained in Roswell Park Memorial Institute (RPMI) 1640 medium, supplemented with 10% fetal bovine serum (FBS) and 10-μg/ml gentamycin. Cells were cultured for less than 6 months after receipt and tested regularly for *Mycoplasma* using the e-Myco™ Mycoplasma PCR detection kit (Intronbio, Seongnam, Korea). Cell lines were authenticated by short tandem repeat analysis of DNA.

Ba/F3 cells were purchased from the Deutsche Sammlung von Mikroorganismen und Zellkulturen (DSMZ) collection (Braunschweig, Germany). *NRAS* wild-type (WT) Ba/F3 cells were maintained in RPMI 1640, supplemented with 10% FBS, 10 μg/ml gentamycin, and interleukin (IL)-3. Ba/F3 cells with *NRAS*-mutations (Q61 K/R/L and G12D) were maintained in RPMI 1640, supplemented with 10% FBS and 10 μg/ml gentamycin, but lacking IL-3.

Pan-RAF inhibitors (LY3009120 and LXH254), dabrafenib, alisertib, and volasertib were purchased from Selleckchem (Boston, MA, USA). Belvarafenib, a pan-RAF inhibitor, was purchased from Chemietek (Indianapolis, IN, USA). Antibodies against total ERK (#9102), phospho (p)-ERK (#9106), total AKT (#4685), p-AKT (#4060S), total EGFR (#4267S), p-EGFR (#3777S), total MEK (#4694S), p-MEK (#9154S), and β-actin (#3700) were purchased from Cell Signaling Technology (Danvers, MA, USA).

2.2. Transduction

Coding sequences for *NRAS*-WT and mutant clones were inserted to the pBABE-puro vector (Addgene, Watertown, MA, USA), and plasmids were transfected into HEK-293FT cells using FuGENE 6 Transfection Reagent (Promega, Madison, WI, USA). After 48 h, viral supernatant was harvested and applied to Ba/F3 cells for 24 h. Virus-infected Ba/F3 cells were selected with puromycin for 2 weeks, and *NRAS*-WT and mutant cells were cultured in the presence and absence of IL-3, respectively. Cloned genes were confirmed by Sanger sequencing.

2.3. Cell proliferation and long-term cell viability assays

Patient-derived NSCLC cell lines and transduced Ba/F3 cell lines were seeded at 3×10^3 cells per well into 96-well plates. IL-3 was added to *NRAS*-WT Ba/F3 cell cultures. After 16 h, cells were treated and incubated for an additional 72 h. The CCK-8 assay (Dojindo, Tokyo, Japan) was used to detect cell proliferation, with absorbance at 450 nm measured using a BioTek (Winooski, VT, USA) microplate reader. Half-maximal inhibitory concentration (IC_{50}) values were calculated by SigmaPlot 12.0 (Systat Software Inc, San Jose, CA, USA). For long-term viability assays, *NRAS*-mutant NSCLC cells were seeded into 12-well plates and treated with LXH254 and volasertib for 7–21 days with media changed every 3 days. Starting cell numbers were established with 80% confluence in the control group on day 14. Colonies were washed with phosphate-buffered saline (PBS), fixed in absolute ethanol, and stained using 0.1% Coomassie Brilliant Blue-R250. Images were captured using the EVOS® Cell Imaging System (Thermo Fisher Scientific, Waltham, MA, USA).

2.4. Western blotting

Cell lysates were harvested in lysis buffer (Cell Signaling Technology), containing Phosphatase Inhibitor, phenylmethylsulfonyl fluoride (PMSF), and Protease Inhibitor Cocktail (Sigma-Aldrich, St. Louis, MO). Equivalent amounts of proteins were resolved by sodium dodecyl sulfate-polyacrylamide gel electrophoresis (SDS-PAGE) using precast gels (Thermo Fisher Scientific). Membranes were incubated with ECL blotting reagents (GE Healthcare, Chicago, IL, USA), and bands were visualized with the Image Quant LAS-4000 Mini (GE Healthcare).

2.5. PCR and sequencing

Genomic DNA was isolated from human NSCLC cell lines or transduced Ba/F3 cells using the QIAamp DNA Blood Midi Kit (QIAGEN, Hilden, Germany), and *NRAS* exons were amplified using the PCR master mix (Lucigen, Middleton, WI, USA). PCR products were purified with the Wizard® Genomic DNA Purification Kit (Promega) and sequenced by Sanger sequencing with primers specific for *NRAS* exons 2 and 3 (listed in Supplementary Table S1).

2.6. Human kinome siRNA library screening

NRAS-mutant NSCLC cells were seeded at 1×10^3 cells per well int 384-well plates. These were transfected with four different small-interfering (si)RNAs targeting 709 human protein kinases (Dharmacon, Lafayette, CO, USA) at a final concentration of 15 nM (3.75 nM each siRNA) using Lipofectamine RNAi-MAX Reagent (Thermo Fisher Scientific). After 48 h, transfected cells were treated with LXH254 at the determined IC_{50} concentration, incubated for an additional 24 h, and analyzed by the Cell Titer-Glo® Luminescent Cell Viability Assay (Promega).

2.7. Human kinome CRISPR knockout library screening

The human kinome CRISPR pooled library (Brunello) was a gift from John Doench and David Root (Addgene #1000000083) [18]. For lentiviral production, human kinome CRISPR library plasmids constructed using the psPAX2 (gift from Didier Trono; Addgene plasmid #12260) and pCMV-VSV-G (gift from Bob Weinberg; Addgene plasmid #8454) vectors were transfected into HEK-293FT cells using Lipofectamine 2000 (Thermo Fisher Scientific). Viral supernatants were harvested and concentrated using Lenti-X Concentrator (Takara, Kusatsu, Japan). Human NSCLC cells were infected with the CRISPR lentiviral library at a multiplicity of infection (MOI) of 0.3 and 8 μg/ml polybrene in T225 plates. After incubation for 1 day, cells were transferred to fresh media containing puromycin and selected for 3 days. Puromycin-resistant cells were split into two conditions, with vehicle or with LXH254 at the IC_{20} concentration, and incubated for 14 days. Residual Genomic DNA of residual cells was extracted using the QIAamp DNA Blood Mini Kit (QIAGEN), and single-guide (sg)RNA was amplified by PCR with Illumina primers (Supplementary Table S1). PCR amplicons were gel-extracted, quantified, and sequenced using the HiSeq 2500 (Illumina, San Diego, CA, USA), and sgRNA frequencies were calculated

using the MAGeCK algorithm [19].

2.8. Cell cycle analysis

NRAS-mutant NSCLC cells were seeded at 2×10^5 cells per well into 6-well plates. After incubation for 16 h, cells were treated with 10-nM volasertib and 1-μM LXH254 for 24 h. Following treatment, the cells were washed with PBS, fixed in 75% cold ethanol, and incubated for 30 min with RNAse A (Sigma-Aldrich) and propidium iodide (PI) (Sigma-Aldrich) at room temperature. Cell cycle analysis was performed with a FACSCalibur flow cytometer (BD Biosciences, San Jose, CA, USA) and FlowJo v.10.6.1 software.

3. Results

3.1. NRAS-mutant Ba/F3 cell lines are sensitive to pan-RAF inhibitors

Ba/F3 cell lines were transduced with vectors expressing *NRAS*-WT and mutant (Q61K, Q61R, Q61L, and G12D) proteins and treated with the pan-RAF inhibitors LY3009120, LXH254, and belvarafenib. Although *NRAS*-WT clones survived only in the presence of IL-3, *NRAS*-mutant-Ba/F3 cells grew spontaneously without IL-3, suggesting oncogenic potential (Supplementary Fig. S2A). Successful transduction was further confirmed by Sanger sequencing, which showed the G12D mutation on *NRAS* exon 2 and the Q61 alterations (Q61K, Q61R, and Q61L) on *NRAS* exon 3 (Fig. 1A). *NRAS*-mutant Ba/F3 cells were more sensitive to pan-RAF inhibitors than dabrafenib, the BRAF specific inhibitor. In addition, cell viability assays revealed that unlike *NRAS*-WT Ba/F3 cells, *NRAS*-mutant Ba/F3 cells are susceptible to LY3009120, LXH254, and belvarafenib treatment. LY3009120 showed similar efficacies against *NRAS*-mutant cells, regardless of subtype. However, cells expressing *NRAS* Q61R, Q61L, and G12D display increased sensitivity to LXH254, compared to *NRAS* Q61K (Fig. 1B). IC_{50} values for LY3009120 (>30 fold), LXH254 (>100 fold), and belvarafenib were further found to be higher for *NRAS*-WT relative to *NRAS*-mutant Ba/F3 cells (Fig. 1C). These results indicate that pan-RAF inhibitors can significantly inhibit cell proliferation, suggesting a possible dependency on the NRAS pathway.

3.2. NRAS-mutant lung cancer cell lines are moderately sensitive to pan-RAF inhibitors and resistant to BRAF inhibitor

We next selected four patient-derived *NRAS*-mutant NSCLC cell lines harboring either the *NRAS* Q61K (HCC15, NCI–H1299, and H2087) or *NRAS* Q61L (HCC1195) mutations. To determine the efficacy of pan-RAF inhibitors against these *NRAS*-mutant cell lines, cell viability assays were performed following treatment with LY3009120, LXH254, belvarafenib, or dabrafenib. We found that *NRAS*-mutant NSCLC cells and Ba/F3 cells display differential sensitivities to the pan-RAF inhibitors. In particular, *NRAS*-mutant NSCLC cells are resistant to dabrafenib (IC_{50}s > 10 μM), and these cells, except HCC1195, display only moderate sensitivity to other pan-RAF inhibitors (IC_{50}s of LY3009120 or LXH254 = 0.5–2.5 μM). HCC1195 were sensitive to pan-RAF inhibitors (IC_{50}s = 0.025–0.1 μM) (Fig. 2A and B). These data suggest that pan-RAF inhibitors are only moderately effective against *NRAS*-mutant NSCLC cell lines.

We then measured levels of RAS pathway-related mRNAs and proteins by quantitative reverse transcription PCR (qRT-PCR) and western blot, respectively, to characterize the pathway dependencies of *NRAS*-mutant NSCLC cells. We detected high levels of EGFR mRNA and pEGFR in NCI–H2087 cells, whereas the highest levels of AKT mRNA and protein were measured in NCI–H1299 cells. Similar molecular heterogeneities were observed in mRNA expression data from the Cancer Cell Line Encyclopedia (CCLE; Supplementary Fig. S2B–D). We further screened tyrosine-phosphorylated receptors using the Human Phospho-RTK Array Kit to determine whether other receptor tyrosine kinases (RTKs) are involved in growth of *NRAS*-mutant NSCLC cells. Our data reveal elevated expression of EGFR in NCI–H2087 cells, although other RTKs were not found to be highly expressed in these cells (Supplementary Fig. S2E). Taken together, these data indicate that *NRAS*-mutant NSCLC cells display heterogeneous molecular profiles, regardless of *NRAS* substitution subtype, which may underlie the limited efficacy of pan-RAF inhibitors.

We further detected increased p-ERK expression after exposure to 1 μM LXH254 in NCI–H1299 and NCI–H2087 cells, suggesting the possibility of an ERK rebound phenomenon (Fig. 2C). The presence of molecular heterogeneity and paradoxical ERK reactivation suggests that a combination strategy is needed to improve efficacy of pan-RAF inhibitors against *NRAS*-mutant NSCLC cells. Because the LY3009120 trial was terminated early (NCT02014116) [16] and belvarafenib showed relatively high IC_{50} concentrations, LXH254 was chosen for further investigation in this study.

3.3. Human kinome siRNA screening identifies PLK1 as a therapeutic target in NRAS-mutant NSCLC cells

The above data demonstrate that LXH254 monotherapy is insufficient for inhibiting growth of *NRAS*-mutant NSCLC cell lines. Therefore, we screened *NRAS*-mutant NSCLC cells with or without LXH254 treatment using a SMARTpool siRNA library consisting of four siRNAs targeting 709 human protein kinases. The siRNA-transfected cells were treated with LXH254 or control vehicle, and growth was analyzed (Fig. 3A). Fig. 3B shows the signal dependencies (defined as relative cell viability <80%) for various kinases, which differed among the cell lines tested (Supplementary Table S2). The four kinases for which deletion most strongly inhibits cell growth from each line are listed in Supplementary Fig. S3A. In addition, genes identified as essential for cell survival differed among the human *NRAS*-mutant NSCLC lines, suggesting heterogeneity of kinase signaling dependency (Supplementary Fig. S3B and C). Notably, only *PLK1* was detected in all LXH254 non-treated groups (Fig. 3B). Knockdown of *PLK1*, one of the 20 common genes identified in the LXH254-treated groups, results in the lowest relative cell viability, and PLK1 is involved in various protein-protein interactions with other kinases (Fig. 3C). Gene set enrichment analysis (GSEA) [20,21] and gene ontology (GO) [22] enrichment score ($P < 0.01$) were used to assess these 20 common genes. Results suggest that the reduced proliferation of *NRAS*-mutant NSCLC cells knocked down for these genes may result from G2/M-phase inhibition (Fig. 3D).

3.4. Human kinome CRISPR knock-out screening identifies PLK1 as a therapeutic target in NRAS-mutant NSCLC cells

We next performed loss-of-function screens for kinases in *NRAS*-mutant NSCLC cells using a lentiviral CRISPR/Cas9 kinome library [18]. We generated a pooled lentivirus library containing the puromycin-resistance gene, Cas9 gene, and sgRNAs for kinase knockouts. After lentivirus-infected cells were selected using puromycin (Day 0), each cell had a loss-of-function mutation for a specific gene mediated by the corresponding sgRNA. Pooled cells were then treated with vehicle (Day 14) or LXH254-containing media at the IC_{20} concentration for 14 days, and sgRNA frequencies were estimated by next-generation sequencing (Fig. 4A). Genes were considered candidate therapeutic targets if two or more corresponding sgRNAs were depleted >50% compared to control cells, as their knockout likely results in cell depletion *via* growth inhibition or cell death. Comparison of sgRNA frequencies for Day 14 cells in vehicle-containing media to those of Day 0 cells (Day 14 *vs.* Day 0) revealed 147 candidate target genes in HCC15, four in NCI–H1299, 68 in NCI–H2087, and 367 in HCC1195 cells (Fig. 4B and Supplementary Fig. S4A). A total of 56 genes, including *PLK1*, were identified in three or more cell lines (Fig. 4B and Supplementary Table S2), and the 'G2M checkpoint' gene set from the hallmark gene sets [20] was significantly enriched in this group (Fig. 4C). When

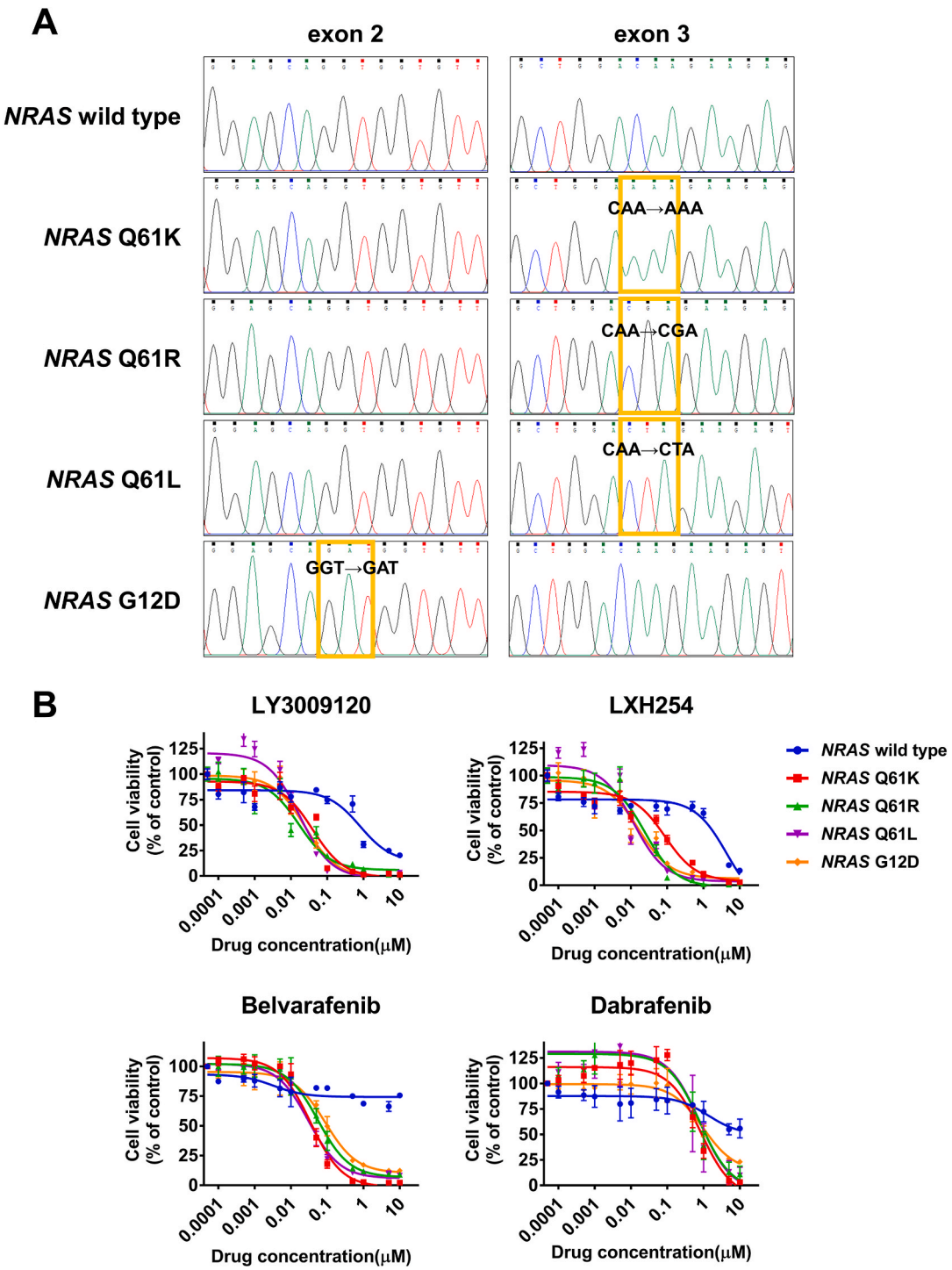

C

IC_{50} (μM)

	LY3009120	LXH254	Belvarafenib	Dabrafenib
***NRAS* wt**	0.77±0.05	2.16±0.6	>10	>10
***NRAS* Q61K**	0.02±0.02	0.05±0.02	0.04±0.008	0.83±0.18
***NRAS* Q61R**	0.02±0.02	0.03±0.02	0.07±0.01	0.97±0.35
***NRAS* Q61L**	0.02±0.02	0.007±0.001	0.04±0.007	0.55±0.12
***NRAS* G12D**	0.02±0.02	0.01±0.002	0.1±0.02	1.15±0.23

(caption on next page)

Fig. 1. *NRAS*-mutant Ba/F3 cells are more sensitive to pan-RAF inhibitors than *NRAS*-wild type (WT) Ba/F3 cells. (A) Construction of *NRAS*-WT and -mutant Ba/F3 cell lines. *NRAS* mutations were verified on exons 2–6 using Sanger sequencing. Yellow box indicates location of the cloned alterations. (B) Cell viability assays were performed on transduced Ba/F3 cells. *NRAS*-WT and -mutant Ba/F3 cells were seeded in media with and without IL-3, respectively, and treated with LY3009120, LXH254, belvarafenib, or dabrafenib for 72 h. Graphs show cell viability of each Ba/F3 cell line throughout the course of treatment with each inhibitor. (C) Table shows IC_{50} values for pan-RAF inhibitors and BRAF inhibitor in Ba/F3 cell lines. All experiments were performed in three independent replicates, and IC_{50} values represent the mean ± standard deviation (SD). (For interpretation of the references to colour in this figure legend, the reader is referred to the Web version of this article.)

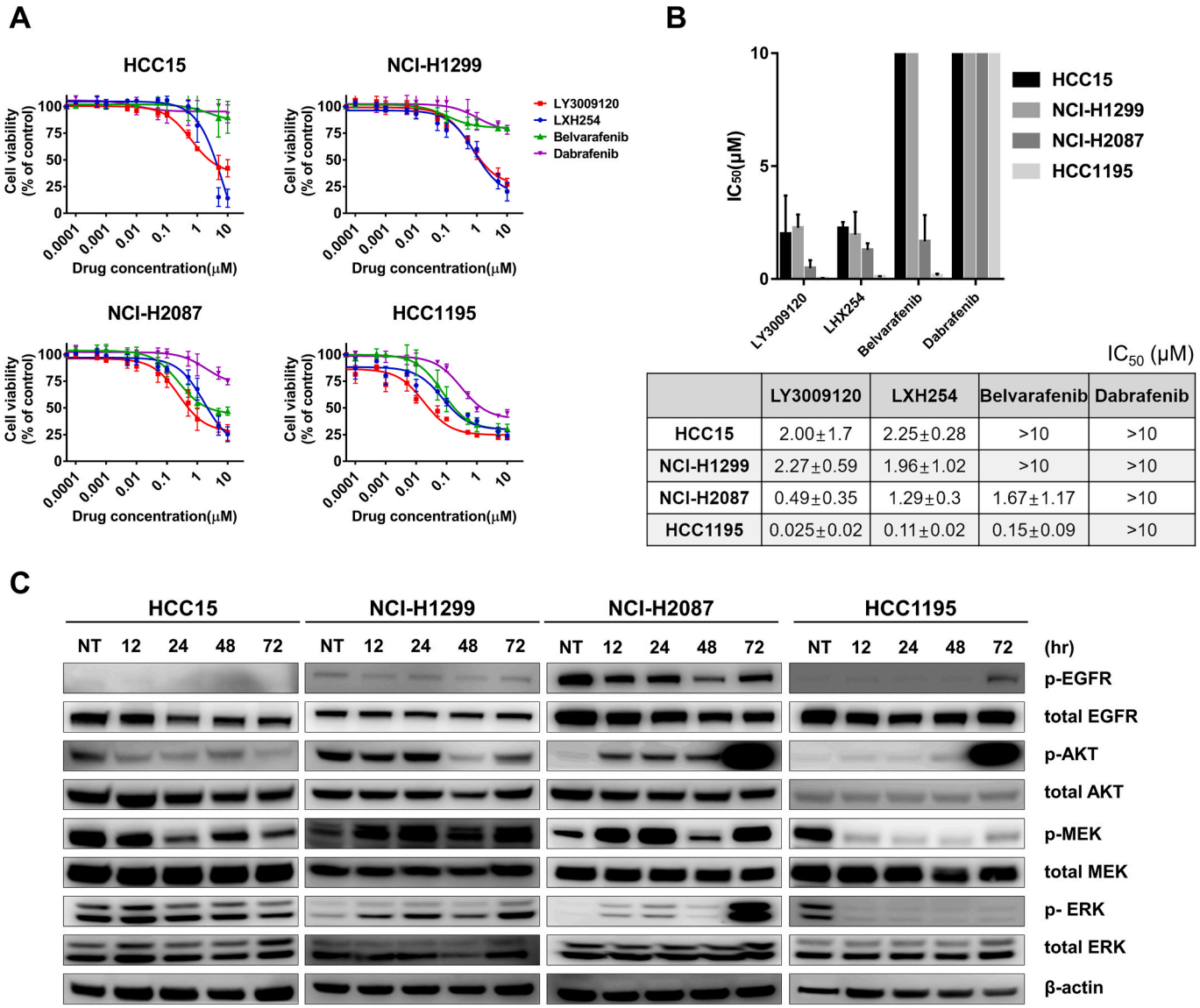

IC_{50} (μM)

	LY3009120	LXH254	Belvarafenib	Dabrafenib
HCC15	2.00±1.7	2.25±0.28	>10	>10
NCI-H1299	2.27±0.59	1.96±1.02	>10	>10
NCI-H2087	0.49±0.35	1.29±0.3	1.67±1.17	>10
HCC1195	0.025±0.02	0.11±0.02	0.15±0.09	>10

Fig. 2. *NRAS*-mutant NSCLC cells show modest sensitivity to pan-RAF inhibitors. (A) Cell viability assays were performed for *NRAS*-mutant NSCLC cells treated with LY3009120, LXH254, belvarafenib, or dabrafenib for 72 h. (B) IC_{50} values shown in (A) were calculated by SigmaPlot 12.0. All experiments were performed in three independent replicates, and the data are depicted as the mean ± SD. (C) Lysates from cells treated with 1 μM LXH254 were analyzed by western blot. NT, no treatment.

sgRNA frequencies for LXH254-treated cells were compared to those of Day 14 cells in vehicle-containing media (LXH254 *vs.* Day 14), we identified 97 candidate target genes in HCC15, 0 in NCI–H1299, 10 in NCI–H2087, and 353 in HCC1195 cells (Fig. 4B and Supplementary Fig. S4B). A total of 59 genes, including *PLK1*, were found in two or more cell lines (Fig. 4B), and the 'G2M checkpoint' gene set from the hallmark gene sets was also significantly enriched in this group (Fig. 4C). In addition, network analysis using the Reactome pathway identified *PLK1* as a hub gene from the 'Cell cycle, mitotic' gene set in control and LXH254-treated cells (Fig. 4D and Supplementary Fig. S4C).

3.5. Combined blockade of PLK1 and pan-RAF is more effective than pan-RAF inhibitor monotherapy against NRAS-mutant NSCLC cells

We then performed cell cycle analysis to confirm that inhibition of PLK1, a key regulator of mitosis, leads to G2/M-phase arrest in *NRAS*-mutant NSCLC cells. Volasertib, a PLK1 inhibitor, induces G2/M-phase arrest in a dose-dependent manner in cancer cells [23,24]. Similarly, we found that low concentrations of volasertib arrest the G2/M-phase in *NRAS*-mutant NSCLC cells. Further, combined inhibition of PLK1 and pan-RAF is more effective in producing G2/M-phase arrest than

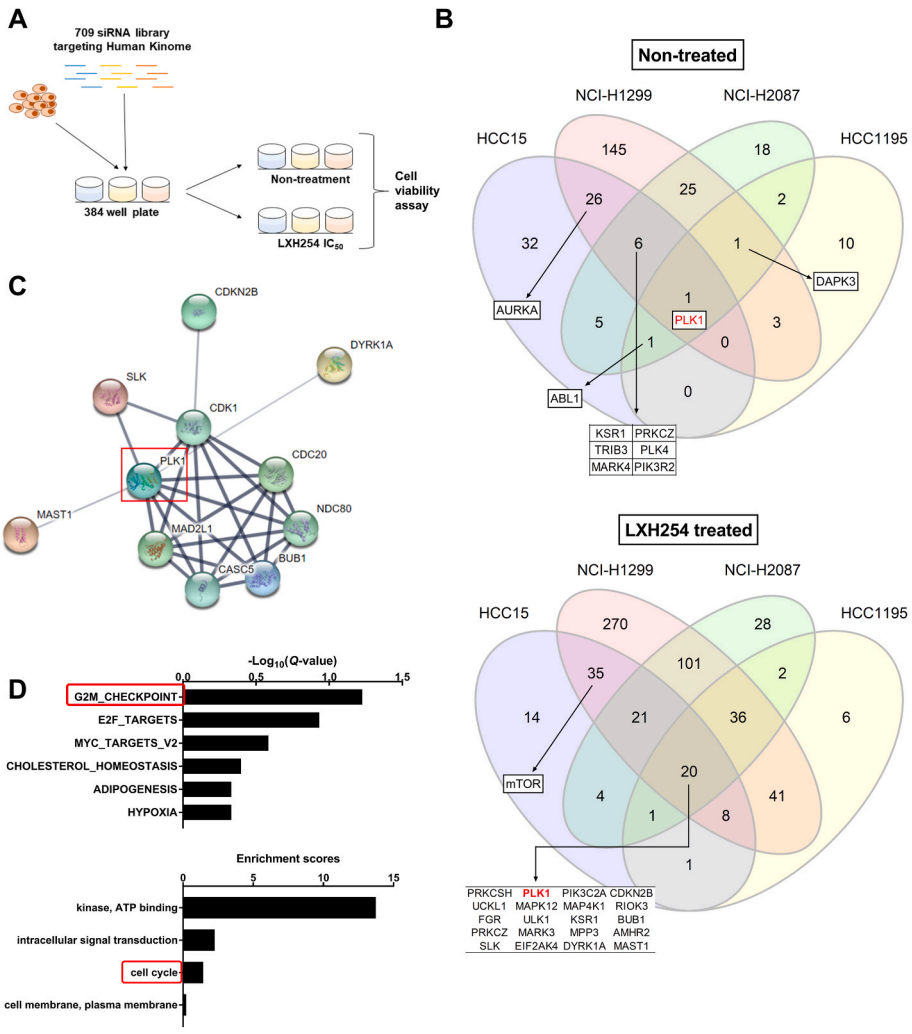

Fig. 3. Screening with a human kinome siRNA library reveals potential targets for enhancing the efficacy of LXH254. (A) Diagram depicting the genome screening method using an siRNA library that targets the human kinome. After LXH254 treatment, viability of transfected cells was measured. (B) Venn diagram of genes whose loss-of-function results in decreased viability following vehicle (top panel) and LXH254 treatment (bottom panel). Gene knockdowns with a relative viability <80% compared to control cells were considered to be candidate targets. (C) Nodes and lines represent proteins and protein-protein interactions, respectively. Line thickness represents confidence according to the STRING dataset (21). The red box highlights PLK1, which resides at a hub of nodes in the network. (D) Gene ontology (GO) annotation was performed on the common genes found in the LXH254-treated group, and enrichment scores were determined by DAVID Functional Annotation Analysis ($P < 0.01$). (For interpretation of the references to colour in this figure legend, the reader is referred to the Web version of this article.)

treatment with LXH254 or volasertib alone (fold-change of G2 cells ranged from 1.75 to 5.9) in all *NRAS*-mutant NSCLC cells, except HCC1195 (Fig. 5A). To further test whether combined volasertib and LXH254 treatment displays synergistic long-term efficacy against *NRAS*-mutant NSCLC cells, we assessed long-term viability of treated cells for 7–21 days. Although no differences in colony formation were observed until Day 7, colony formation differed significantly between cells treated individually with volasertib or LXH254 and those subjected to combined therapy after 14 days. In particular, inhibition of cell growth was maintained only in the combined therapy group, and long-term efficacy of volasertib and LXH254 was dependent on the dose of LXH254 administered. Although dual blockade of PLK1 and pan-RAF displayed a modest effect than volasertib monotherapy in short-term cell proliferation, this showed a synergistic effect in the long-term viability assay (Fig. 5C, Supplementary Fig. S5A and S5B). Taken together, these data suggest that combined therapy can overcome resistance to volasertib or LXH254 monotherapy in drug-tolerant states that may develop during treatment.

4. Discussion

In this study, we show that *NRAS* mutant-expressing Ba/F3 cells are highly sensitive to pan-RAF inhibitors, whereas *NRAS*-mutant NSCLC cell lines are only moderately sensitive to these therapeutics. Because molecular heterogeneity and ERK rebound may contribute to the observed limited efficacy of pan-RAF inhibitor monotherapy, a combination strategy may be necessary to inhibit growth of *NRAS*-mutant NSCLC cells. Accordingly, kinome-wide screenings revealed that cell cycle inhibition is lethal to *NRAS*-mutant NSCLC cell lines, and combination treatment with pan-RAF plus PLK1 inhibitors displays superior long-term efficacy against *NRAS*-mutant NSCLC cell lines.

NRAS mutation is found in 28% of melanoma patients [25], and other than MEK inhibition, no other therapies have been approved for treating *NRAS*-mutant melanoma. However, in a previous study, MEK inhibition with binimetinib alone showed superior, but limited, clinical outcomes compared with dacarbazine in patients with advanced *NRAS*-mutant melanoma (median progression-free survival, 2.8 *vs.* 1.5 months, $P < 0.001$) [26]. Several studies have also reported that RAF inhibitors either alone or in combination with MEK or CDK4/6 inhibitor are effective for treating *RAS*-mutant cancers, but not *NRAS*-mutant NSCLC [27–30]. Here, we demonstrate that pan-RAF inhibitors, including LY3009120, LXH254, and belvarafenib, can inhibit proliferation of *NRAS*-mutant expressing Ba/F3 cells. However, patient-derived *NRAS*-mutant NSCLC cells with heterogeneous molecular profiles and ERK reactivation after pan-RAF inhibitor treatment show only moderate sensitivity to pan-RAF inhibitor monotherapy. This was observed for all *NRAS*-mutant NSCLC cell lines examined except HCC1195 cells, which lack ERK reactivation. Similarly, our patient with advanced $NRAS^{G13R}$-mutant NSCLC who received Type II pan-RAF inhibitor monotherapy exhibited a prolonged, stable condition (Supplementary Fig. S1).

We therefore performed kinome-wide siRNA and CRISPR/Cas9

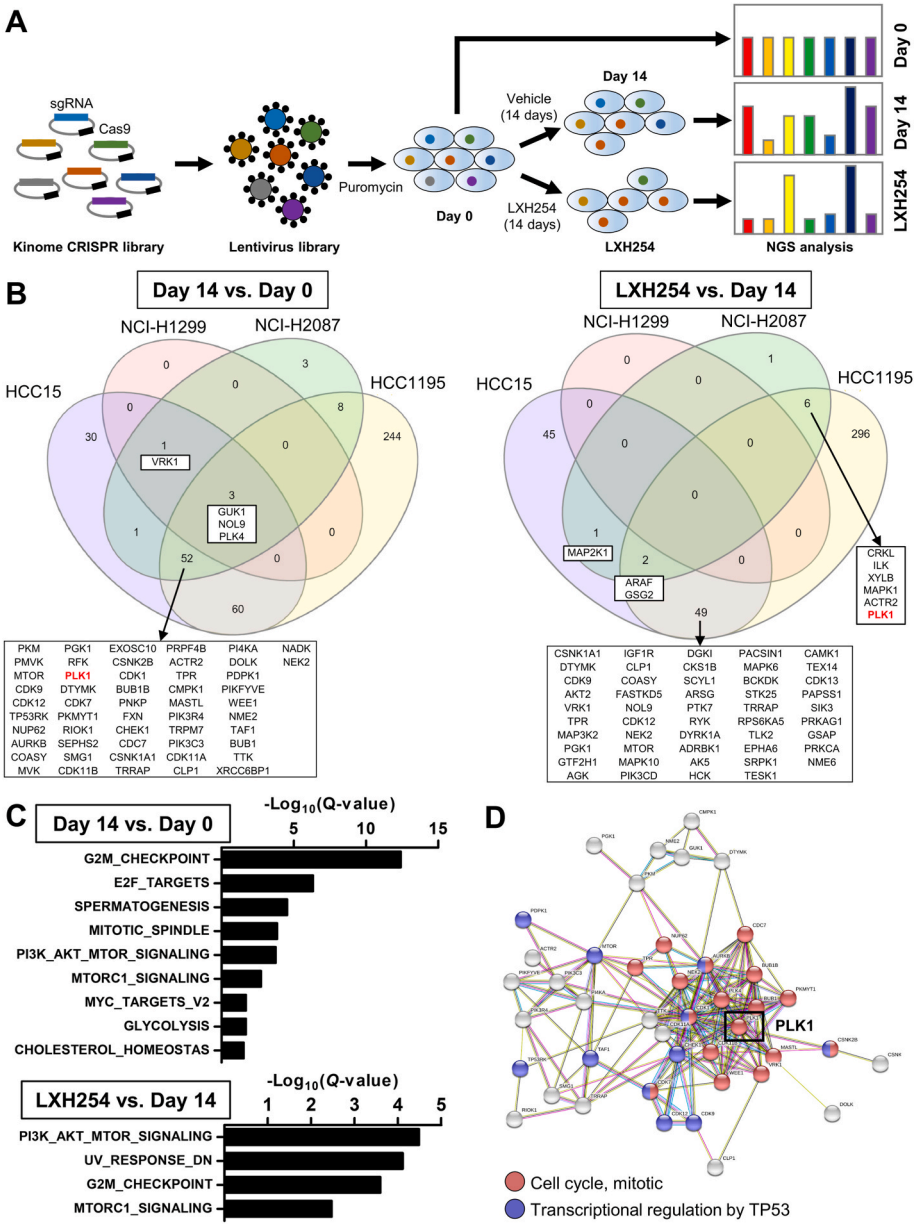

Fig. 4. Human kinome CRISPR screening for potential therapeutic targets in *NRAS*-mutant NSCLC cells. (A) Schematic showing the human kinome CRISPR knock-out screens for identifying genes whose loss-of-function decreases cell viability in *NRAS*-mutant NSCLC cells. Lentiviral kinome CRISPR library-infected cells (Day 0), comprised of a mixture of cells with specific loss-of-function mutations mediated by corresponding single-guide (sg)RNAs, were selected in vehicle (Day 14) or LXH254-containing media (LXH254) for 14 days. The sgRNA frequencies were estimated from residual cells (Day 0, Day 14, and LXH254) using next-generation sequencing (NGS). (B) Venn diagram of genes whose loss-of-function results in cell depletion following vehicle (left panel) and LXH254 treatment (right panel). Left panel shows the number of genes whose sgRNA were depleted in Day 14 cells treated with vehicle-containing media compared to Day 0 cells (Day 14 *vs.* Day 0). Right panel shows the number of genes whose sgRNAs were depleted in LXH254-treated cells compared to Day 14 cells treated with vehicle-containing media (LXH254 *vs.* Day 14). Genes were regarded as candidate targets when two or more sgRNAs were depleted by > 50% compared to control cells. (C) Gene set analysis of candidate target genes from vehicle (Day 14 *vs.* Day 0, upper panel) and LXH254-treated cells (LXH254 *vs.* Day 14, lower panel) using the hallmark gene set of the Molecular Signature Database. Significantly enriched gene sets (false discovery rate [FDR] Q < 0.01) for the 56 genes from vehicle treatment (Day 14 *vs.* Day 0; commonly found in three or more cells) and the 59 genes from LXH254-treatment (LXH254 *vs.* Day 14; commonly found in two or more cells) are depicted. (D) STRING network analysis of the 56 genes depleted in the vehicle-treated group (Day 14 *vs.* Day 0). Genes involved in cell cycle progression and transcriptional regulation by *TP53* are indicated in red and blue, respectively. PLK1 is a one of the hub nodes in the network and is indicated by a black box. (For interpretation of the references to colour in this figure legend, the reader is referred to the Web version of this article.)

knockout screens in *NRAS*-mutant NSCLC cells in the presence and absence of LXH254 to identify kinases that promote NSCLC survival and may represent possible therapeutic targets. Our results show that PLK1 inhibition is associated with G2/M-phase arrest ('polo-arrest') and disrupts growth of *NRAS*-mutant NSCLC cells. PLK1 is an important regulator of mitotic initiation [31]. Its overexpression can promote tumorigenesis, and increased expression of PLK1 has been detected in human cancers, particularly lung adenocarcinoma, relative to normal tissues (fold-change, 9.7) [32]. Here, we found that dual blockade of pan-RAF and PLK1 shows potent efficacy against *NRAS*-mutant NSCLC cells, particularly HCC15 and HCC1195 cells, and combined inhibition of PLK1 and pan-RAF decreases cell growth *via* cell cycle arrest at the G2/M phase. Furthermore, cell growth in long-term viability assays is inhibited by volasertib and LXH254 combined treatment, as compared to volasertib or LXH254 monotherapy. Collectively, these data suggest that combined blockade of PLK1 and pan-RAF may represent an effective, alternative therapy to combat resistance to pan-RAF inhibitor monotherapy in *NRAS*-mutant NSCLC. Notably, although RAF inhibitor plus CDK4/6 inhibitor displays synergistic activity against *NRAS*-mutant melanoma by arresting cell cycle progression at the G0/G1 phase [29,30], CDK4 and CDK6 were not uncovered in our kinome-wide siRNA screening of *NRAS*-mutant NSCLC cells. In addition, dual blockade of PLK1 and MEK produces a synergistic effect in *NRAS*-mutant melanoma models *in vitro* and *in vivo* [33]. Taken together, our results show that dual blockade of PLK1 and pan-RAF may be a promising treatment strategy for patients with *NRAS*-mutant NSCLC. However, these *in vitro* data should be validated in an *in vivo* patient-derived xenograft model of *NRAS*-mutant NSCLC.

Interestingly, pan-RAF inhibition alone activated AKT signaling in NCI–H2087 and HCC1195 cells. In addition, although there was no significant activation of the mTOR after LXH254 treatment, combined blockade of mTOR and PLK1 displayed a modest synergistic effect against *NRAS*-mutant NSCLC in 72 h viability assay (data not shown). These data suggest that AKT/mTOR pathway might bypass the MAPK pathway in *NRAS*-mutant NSCLC cells treated with pan-RAF inhibitor. Furthermore, we found that the *NRAS*-mutant NSCLC cell lines treated with LXH254 and volasertib were vulnerable to the knockdown of PI3K/AKT/mTOR signaling pathways using the Kinome siRNA library

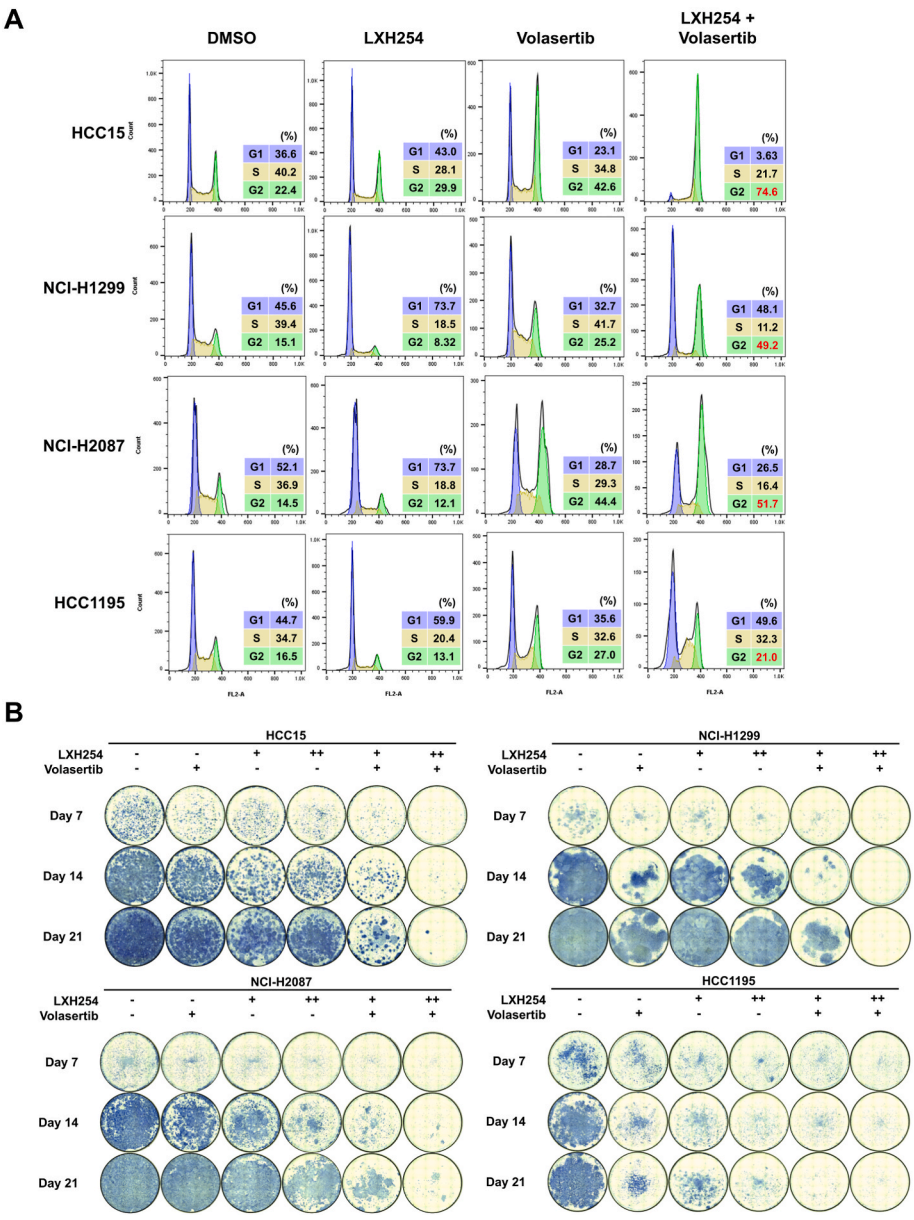

Fig. 5. Combined blockade of PLK1 and pan-RAF reduces the viability of *NRAS*-mutant cells. (A) Cell cycle progression of *NRAS*-mutant cells was analyzed after drug treatment. Cells were treated for 24 h with 10-nM volasertib, 1-μM LXH254, or both in combination before propidium iodide (PI) staining, followed by flow cytometric analysis. The graphs shown represent results from three independent experiments. (B) *NRAS*-mutant cells treated with control (DMSO), volasertib (5 nM; +), and LXH254 (0.5 μM; + or 1 μM; ++) were stained by Coomassie Brilliant Blue-R250 at days 7, 14, and 21. (For interpretation of the references to colour in this figure legend, the reader is referred to the Web version of this article.)

screening (data not shown), suggesting the dependency of PI3K/AKT/mTOR pathway in the short-term inhibition of pan-RAF and PLK1. In addition, although PI3K/AKT/mTOR signaling kinases comprise a major cluster in the protein-protein network of genes depleted by LXH254 treatment using CRISPR/Cas9, the combination treatment with AZD5363, an AKT inhibitor, and LXH254 does not synergistically inhibit the growth of *NRAS*-mutant NSCLC cells in either 72 h or long-term viability assays (Supplementary Fig. S4, S5C, and S5D). Taken together, the pathway dependency of PI3K/AKT/mTOR might be stronger in the combination treatment than LXH254 monotherapy, implying a compensatory mechanism in short-term viability assays.

In conclusion, we found that treatment with LXH254, a pan-RAF inhibitor, is insufficient for inhibiting *NRAS*-mutant NSCLC cell proliferation due to molecular heterogeneity and ERK reactivation. However, inhibition of cell cycle mediators, especially PLK1, in combination with LXH254, leads to synergistic inhibition of *NRAS*-mutant NSCLC cell growth. Our preclinical results might support LXH254-centric combination trials for treating *NRAS*-mutant cancers (NCT02607813 and NCT02974725). These data warrant further investigation to develop a novel therapeutic strategy that incorporates PLK1 and pan-RAF inhibitors for treating patients with advanced *NRAS*-mutant NSCLC.

Author contributions

Conceptualization: T.M. Kim, S.Y. Cho, S. Park.
Methodology: S. Park, S. Kim, Y. Oh.
Acquisition of data: S. Park, T.M. Kim, S.Y. Cho, S. Kim, Y. Oh, M. Kim, B. Keam, D.W. Kim, D.S. Heo.
Analysis and interpretation of data: S. Park, T.M. Kim, S.Y. Cho, S. Kim, Y. Oh, M. Kim, B. Keam, D.W. Kim, D.S. Heo.
Writing: S. Park, T.M. Kim, S.Y. Cho.
Supervision: T.M. Kim, S.Y. Cho.

Declaration of competing interest

Dr. Kim received grants from AstraZeneca-KHIDI outside this work. The other authors declare no potential conflicts of interest.

Acknowledgments

This study was supported by grants from the Korean Health Technology R&D Project “Strategic Center of Cell and Bio Therapy for Heart, Diabetes & Cancer” through the Korea Health Industry Development Institute (KHIDI), funded by the Ministry of Health & Welfare (MHW) (grant number: HI-17C-2085), as well as the Bio & Medical Technology Development Program of the National Research Foundation (NRF), funded by the Korean government (MSIT) (grant number: NRF-2018M3A9F3056902 and NRF-2019M3E5D4066900).

Appendix B. Supplementary data

Supplementary data related to this article can be found at https://doi.org/10.1016/j.canlet.2020.09.018.

Abbreviations

CI	combination index
FBS	fetal bovine serum
GESA	Gene set enrichment analysis
GO	Gene ontology
IC_{50}	Half-maximal inhibitory concentration
IL-3	Interleukin-3
MOI	multiplicity of infection
NSCLC	Non-small cell lung cancer
p-ERK	phosphorylated ERK
p-AKT	phosphorylated AKT
p-EGFR	phosphorylated EGFR
p-MEK	phosphorylated MEK
PBS	phosphate buffered saline
PI	propidium iodide
PLK1	Polo-like kinase 1
PMSF	phenylmethylsulfonyl fluoride
qRT-PCR	Quantitative reverse transcription PCR
RTK	receptor tyrosine kinase
sgRNA	single-guide RNA
siRNA	small interfering RNA
WT	wild-type

References

[1] R.L. Siegel, K.D. Miller, A. Jemal, Cancer statistics, CA Cancer J Clin 69 (2019) 7–34, 2019.
[2] M. Ock, W.J. Choi, M.W. Jo, Trend analysis of major cancer statistics according to sex and severity levels in Korea, PloS One 13 (2018), e0203110.
[3] F. Bray, J. Ferlay, I. Soerjomataram, R.L. Siegel, L.A. Torre, A. Jemal, Global cancer statistics 2018: GLOBOCAN estimates of incidence and mortality worldwide for 36 cancers in 185 countries, CA Cancer J Clin 68 (2018) 394–424.
[4] J. Liu, W. Lee, Z. Jiang, Z. Chen, S. Jhunjhunwala, P.M. Haverty, F. Gnad, Y. Guan, H.N. Gilbert, J. Stinson, C. Klijn, J. Guillory, D. Bhatt, S. Vartanian, K. Walter, J. Chan, T. Holcomb, P. Dijkgraaf, S. Johnson, J. Koeman, J.D. Minna, A.F. Gazdar, H.M. Stern, K.P. Hoeflich, T.D. Wu, J. Settleman, F.J. de Sauvage, R.C. Gentleman, R.M. Neve, D. Stokoe, Z. Modrusan, S. Seshagiri, D.S. Shames, Z. Zhang, Genome and transcriptome sequencing of lung cancers reveal diverse mutational and splicing events, Genome Res. 22 (2012) 2315–2327.
[5] L. Ding, G. Getz, D.A. Wheeler, E.R. Mardis, M.D. McLellan, K. Cibulskis, C. Sougnez, H. Greulich, D.M. Muzny, M.B. Morgan, L. Fulton, R.S. Fulton, Q. Zhang, M.C. Wendl, M.S. Lawrence, D.E. Larson, K. Chen, D.J. Dooling, A. Sabo, A.C. Hawes, H. Shen, S.N. Jhangiani, L.R. Lewis, O. Hall, Y. Zhu, T. Mathew, Y. Ren, J. Yao, S.E. Scherer, K. Clerc, G.A. Metcalf, B. Ng, A. Milosavljevic, M. L. Gonzalez-Garay, J.R. Osborne, R. Meyer, X. Shi, Y. Tang, D.C. Koboldt, L. Lin, R. Abbott, T.L. Miner, C. Pohl, G. Fewell, C. Haipek, H. Schmidt, B.H. Dunford-Shore, A. Kraja, S.D. Crosby, C.S. Sawyer, T. Vickery, S. Sander, J. Robinson, W. Winckler, J. Baldwin, L.R. Chirieac, A. Dutt, T. Fennell, M. Hanna, B.E. Johnson, R.C. Onofrio, R.K. Thomas, G. Tonon, B.A. Weir, X. Zhao, L. Ziaugra, M.C. Zody, T. Giordano, M.B. Orringer, J.A. Roth, M.R. Spitz, Wistuba II, B. Ozenberger, P. J. Good, A.C. Chang, D.G. Beer, M.A. Watson, M. Ladanyi, S. Broderick, A. Yoshizawa, W.D. Travis, W. Pao, M.A. Province, G.M. Weinstock, H.E. Varmus, S.B. Gabriel, E.S. Lander, R.A. Gibbs, M. Meyerson, R.K. Wilson, Somatic mutations affect key pathways in lung adenocarcinoma, Nature 455 (2008) 1069–1075.
[6] K. Ohashi, L.V. Sequist, M.E. Arcila, C.M. Lovly, X. Chen, C.M. Rudin, T. Moran, D. R. Camidge, C.L. Vnencak-Jones, L. Berry, Y. Pan, H. Sasaki, J.A. Engelman, E. B. Garon, S.M. Dubinett, W.A. Franklin, G.J. Riely, M.L. Sos, M.G. Kris, D. Dias-Santagata, M. Ladanyi, P.A. Bunn Jr., W. Pao, Characteristics of lung cancers harboring NRAS mutations, Clin. Canc. Res. 19 (2013) 2584–2591.
[7] E.J. Jordan, H.R. Kim, M.E. Arcila, D. Barron, D. Chakravarty, J. Gao, M.T. Chang, A. Ni, R. Kundra, P. Jonsson, G. Jayakumaran, S.P. Gao, H.C. Johnsen, A. J. Hanrahan, A. Zehir, N. Rekhtman, M.S. Ginsberg, B.T. Li, H.A. Yu, P.K. Paik, A. Drilon, M.D. Hellmann, D.N. Reales, R. Benayed, V.W. Rusch, M.G. Kris, J. E. Chaft, J. Baselga, B.S. Taylor, N. Schultz, C.M. Rudin, D.M. Hyman, M.F. Berger, D.B. Solit, M. Ladanyi, G.J. Riely, Prospective comprehensive molecular characterization of lung adenocarcinomas for efficient patient matching to approved and emerging therapies, Canc. Discov. 7 (2017) 596–609.
[8] D.K. Simanshu, D.V. Nissley, F. McCormick, RAS proteins and their regulators in human disease, Cell 170 (2017) 17–33.
[9] H. Ledford, Cancer: the Ras renaissance, Nature 520 (2015) 278–280.
[10] M.R. Janes, J. Zhang, L.S. Li, R. Hansen, U. Peters, X. Guo, Y. Chen, A. Babbar, S. J. Firdaus, L. Darjania, J. Feng, J.H. Chen, S. Li, S. Li, Y.O. Long, C. Thach, Y. Liu, A. Zarieh, T. Ely, J.M. Kucharski, L.V. Kessler, T. Wu, K. Yu, Y. Wang, Y. Yao, X. Deng, P.P. Zarrinkar, D. Brehmer, D. Dhanak, M.V. Lorenzi, D. Hu-Lowe, M. P. Patricelli, P. Ren, Y. Liu, Targeting KRAS mutant cancers with a covalent G12C-specific inhibitor, Cell 172 (2018) 578–589 e517.
[11] AMG 510 first to inhibit "undruggable" KRAS, Canc. Discov. 9 (2019) 988–989.
[12] S. Vatansever, B. Erman, Z.H. Gumus, Oncogenic G12D mutation alters local conformations and dynamics of K-Ras, Sci. Rep. 9 (2019) 11730.
[13] M.B. Ryan, R.B. Corcoran, Therapeutic strategies to target RAS-mutant cancers, Nat. Rev. Clin. Oncol. 15 (2018) 709–720.
[14] T.W. Kim, J. Lee, S.J. Shin, J.-S. Kim, Y.J. Kim, H.S. Han, S.J. Lee, H.-S. Lim, Y.-h. Hong, Y.S. Noh, Y. Kyoung, O. Han, J. Yoon, J.A. Lim, S.R. Kim, Belvarafenib, a novel pan-RAF inhibitor, in solid tumor patients harboring BRAF, KRAS, or NRAS mutations: phase I study, J. Clin. Oncol. 37 (2019), 3000-3000.
[15] S.B. Peng, J.R. Henry, M.D. Kaufman, W.P. Lu, B.D. Smith, S. Vogeti, T.J. Rutkoski, S. Wise, L. Chun, Y. Zhang, R.D. Van Horn, T. Yin, X. Zhang, V. Yadav, S.H. Chen, X. Gong, X. Ma, Y. Webster, S. Buchanan, I. Mochalkin, L. Huber, L. Kays, G. P. Donoho, J. Walgren, D. McCann, P. Patel, I. Conti, G.D. Plowman, J.J. Starling, D.L. Flynn, Inhibition of RAF isoforms and active dimers by LY3009120 leads to anti-tumor activities in RAS or BRAF mutant cancers, Canc. Cell 28 (2015) 384–398.
[16] D.S. Hong, A. Hollebecque, M.S. Gordon, K.T. Flaherty, G. Shapiro, J. Rodon, M. Millward, N. Ramdas, W. Zhang, L. Gao, A. Sykes, M.D. Willard, D. Yu, A. Schade, D.L. Flynn, M. Kaufman, S.-B. Peng, I. Conti, R.V. Tiu, R.J. Sullivan, A first-in-human dose phase 1 study of LY3009120 in advanced cancer patients 35 (2017), 2507-2507.
[17] D.D. Stuart, W. Shao, Y. Mishina, Y. Feng, G. Caponigro, V.G. Cooke, S. Rivera, F. Shen, J. Korn, L.A.M. Griner, G. Nishiguchi, B. Taft, L. Wan, S. Subramanian, Y. Lou, L. Setti, M. Burger, V. Tamez, A. Rico, R. Aversa, J. Tellew, J.R. Haling, V. Polyakov, A. Lambert, R. Zang, A.V. Abbema, M. Hekmat-Nejad, P. Amiri, M. Singh, N. Keen, M.P. Dillon, E. Lees, W.R. Sellers, S. Ramurthy, Abstract DDT01-04: pharmacological profile and anti-tumor properties of LXH254, a highly selective RAF kinase inhibitor, Canc. Res. 78 (2018). DDT01-04-DDT01-04.
[18] J.G. Doench, N. Fusi, M. Sullender, M. Hegde, E.W. Vaimberg, K.F. Donovan, I. Smith, Z. Tothova, C. Wilen, R. Orchard, H.W. Virgin, J. Listgarten, D.E. Root, Optimized sgRNA design to maximize activity and minimize off-target effects of CRISPR-Cas9, Nat. Biotechnol. 34 (2016) 184–191.
[19] W. Li, H. Xu, T. Xiao, L. Cong, M.I. Love, F. Zhang, R.A. Irizarry, J.S. Liu, M. Brown, X.S. Liu, MAGeCK enables robust identification of essential genes from genome-scale CRISPR/Cas9 knockout screens, Genome Biol. 15 (2014) 554.
[20] A. Subramanian, P. Tamayo, V.K. Mootha, S. Mukherjee, B.L. Ebert, M.A. Gillette, A. Paulovich, S.L. Pomeroy, T.R. Golub, E.S. Lander, J.P. Mesirov, Gene set enrichment analysis: a knowledge-based approach for interpreting genome-wide expression profiles, Proc. Natl. Acad. Sci. U. S. A. 102 (2005) 15545–15550.
[21] V.K. Mootha, C.M. Lindgren, K.F. Eriksson, A. Subramanian, S. Sihag, J. Lehar, P. Puigserver, E. Carlsson, M. Ridderstrale, E. Laurila, N. Houstis, M.J. Daly, N. Patterson, J.P. Mesirov, T.R. Golub, P. Tamayo, B. Spiegelman, E.S. Lander, J. N. Hirschhorn, D. Altshuler, L.C. Groop, PGC-1alpha-responsive genes involved in oxidative phosphorylation are coordinately downregulated in human diabetes, Nat. Genet. 34 (2003) 267–273.
[22] G. Dennis Jr., B.T. Sherman, D.A. Hosack, J. Yang, W. Gao, H.C. Lane, R. A. Lempicki, DAVID: database for annotation, visualization, and integrated discovery, Genome Biol. 4 (2003) P3.
[23] D.W. Zheng, Y.Q. Xue, Y. Li, J.M. Di, J.G. Qiu, W.J. Zhang, Q.W. Jiang, Y. Yang, Y. Chen, M.N. Wei, J.R. Huang, K. Wang, X. Wei, Z. Shi, Volasertib suppresses the growth of human hepatocellular carcinoma in vitro and in vivo, Am J Cancer Res 6 (2016) 2476–2488.
[24] Y. Adachi, Y. Ishikawa, H. Kiyoi, Identification of volasertib-resistant mechanism and evaluation of combination effects with volasertib and other agents on acute myeloid leukemia, Oncotarget 8 (2017) 78452–78465.
[25] N.K. Hayward, J.S. Wilmott, N. Waddell, P.A. Johansson, M.A. Field, K. Nones, A.-M. Patch, H. Kakavand, L.B. Alexandrov, H. Burke, V. Jakrot, S. Kazakoff, O. Holmes, C. Leonard, R. Sabarinathan, L. Mularoni, S. Wood, Q. Xu, N. Waddell, V. Tembe, G.M. Pupo, R. De Paoli-Iseppi, R.E. Vilain, P. Shang, L.M.S. Lau, R. A. Dagg, S.-J. Schramm, A. Pritchard, K. Dutton-Regester, F. Newell, A. Fitzgerald, C.A. Shang, S.M. Grimmond, H.A. Pickett, J.Y. Yang, J.R. Stretch, A. Behren, R. F. Kefford, P. Hersey, G.V. Long, J. Cebon, M. Shackleton, A.J. Spillane, R.P. M. Saw, N. López-Bigas, J.V. Pearson, J.F. Thompson, R.A. Scolyer, G.J. Mann, Whole-genome landscapes of major melanoma subtypes, Nature 545 (2017) 175.
[26] R. Dummer, D. Schadendorf, P.A. Ascierto, A. Arance, C. Dutriaux, A.M. Di Giacomo, P. Rutkowski, M. Del Vecchio, R. Gutzmer, M. Mandala, L. Thomas,

L. Demidov, C. Garbe, D. Hogg, G. Liszkay, P. Queirolo, E. Wasserman, J. Ford, M. Weill, L.A. Sirulnik, V. Jehl, V. Bozón, G.V. Long, K. Flaherty, Binimetinib versus dacarbazine in patients with advanced NRAS-mutant melanoma (NEMO): a multicentre, open-label, randomised, phase 3 trial, Lancet Oncol. 18 (2017) 435–445.

[27] O. Abdel-Wahab, V.M. Klimek, A.A. Gaskell, A. Viale, D. Cheng, E. Kim, R. Rampal, M. Bluth, J.J. Harding, M.K. Callahan, T. Merghoub, M.F. Berger, D.B. Solit, N. Rosen, R.L. Levine, P.B. Chapman, Efficacy of intermittent combined RAF and MEK inhibition in a patient with concurrent BRAF- and NRAS-mutant malignancies, Canc. Discov. 4 (2014) 538–545.

[28] M.A. Bonelli, A. Cavazzoni, F. Saccani, R.R. Alfieri, F. Quaini, S. La Monica, M. Galetti, D. Cretella, C. Caffarra, D. Madeddu, C. Frati, C.A. Lagrasta, A. Falco, P. Rossetti, C. Fumarola, M. Tiseo, P.G. Petronini, A. Ardizzoni, Inhibition of PI3K pathway reduces invasiveness and epithelial-to-mesenchymal transition in squamous lung cancer cell lines harboring PIK3CA gene alterations, Mol. Canc. Therapeut. 14 (2015) 1916–1927.

[29] S.H. Chen, X. Gong, Y. Zhang, R.D. Van Horn, T. Yin, L. Huber, T.F. Burke, J. Manro, P.W. Iversen, W. Wu, S.V. Bhagwat, R.P. Beckmann, R.V. Tiu, S. G. Buchanan, S.B. Peng, RAF inhibitor LY3009120 sensitizes RAS or BRAF mutant cancer to CDK4/6 inhibition by abemaciclib via superior inhibition of phospho-RB and suppression of cyclin D1, Oncogene 37 (2018) 821–832.

[30] L.N. Kwong, J.C. Costello, H. Liu, S. Jiang, T.L. Helms, A.E. Langsdorf, D. Jakubosky, G. Genovese, F.L. Muller, J.H. Jeong, R.P. Bender, G.C. Chu, K. T. Flaherty, J.A. Wargo, J.J. Collins, L. Chin, Oncogenic NRAS signaling differentially regulates survival and proliferation in melanoma, Nat. Med. 18 (2012) 1503–1510.

[31] S. Schmucker, I. Sumara, Molecular dynamics of PLK1 during mitosis, Mol Cell Oncol 1 (2014), e954507.

[32] Z. Liu, Q. Sun, X. Wang, PLK1, A potential target for cancer therapy, Transl Oncol 10 (2017) 22–32.

[33] C. Posch, B.D. Cholewa, I. Vujic, M. Sanlorenzo, J. Ma, S.T. Kim, S. Kleffel, T. Schatton, K. Rappersberger, R. Gutteridge, N. Ahmad, S. Ortiz/Urda, Combined inhibition of MEK and Plk1 has synergistic antitumor activity in NRAS mutant melanoma, J. Invest. Dermatol. 135 (2015) 2475–2483.